

A Stochastic Liouville Equation Approach for the Effect of Noise in Quantum Computations

Y. C. Cheng and R. J. Silbey*

Department of Chemistry and Center for Materials Science and Engineering

Massachusetts Institute of Technology

Cambridge, Massachusetts 02139

We propose a model based on a generalized effective Hamiltonian for studying the effect of noise in quantum computations. The system-environment interactions are taken into account by including stochastic fluctuating terms in the system Hamiltonian. Treating these fluctuations as Gaussian Markov processes with zero mean and delta function correlation times, we derive an exact equation of motion describing the dissipative dynamics for a system of n qubits. We then apply this model to study the effect of noise on the quantum teleportation and a generic quantum controlled-NOT (CNOT) gate. For quantum teleportation, the effect of noise in the quantum channels are found to be additive, and the teleportation fidelity depends on the state of the teleported qubit. The effect of collective decoherence is also studied for the two-qubit entangled states. For the quantum CNOT gate, we study the effect of noise on a set of one- and two-qubit quantum gates, and show that the results can be assembled together to investigate the quality of a quantum CNOT gate operation. We compute the averaged gate fidelity and gate purity for the quantum CNOT gate, and investigate phase, bit-flip, and flip-flop errors during the CNOT gate operation. The effects of direct inter-qubit coupling and fluctuations on the control fields are also studied. We find that the quality of the CNOT gate operation is sensitive to the strengths of the control fields and the strengths of the noise, and the effect of noise is additive regardless of its origin. We discuss the limitations and possible extensions of this model. In sum, we demonstrate a simple model that enables us to investigate the effect of noise in arbitrary quantum circuits under realistic device conditions.

I. INTRODUCTION

Quantum information processing is of much current interest[1]. The realization of quantum algorithms using nuclear magnetic resonance (NMR) [2, 3, 4, 5] and ion-trap [6] techniques has shown that quantum computing is possible in principle. Recent efforts for building quantum com-

*Electronic address: silbey@mit.edu

puters have focused on techniques based on solid-state devices that are believed to be more scalable [7, 8, 9]. However, such solid-state devices usually require sophisticated manufacturing techniques, and the inevitable interactions between a qubit and its surrounding environment (“bath”) introduce noise into the quantum system, resulting in the degradation of the quantum superposition state. Thus, the extra degrees of freedom of a solid-state system and the inherent system-bath interactions pose a great problem for quantum computing with such devices. The decoherence problem is the main obstacle towards the realization of a universal quantum computer, and a sound theoretical framework for the description of the decoherence and population relaxation of qubit systems is necessary [10, 11].

Because the ability to compute and predict the behavior of a quantum circuit under the influence of noise is crucial, a model that can describe errors from the system-bath interactions could be extremely useful. Such a model will also be useful in the study of quantum error-correcting and error-preventing schemes, as well as provide informative guidelines for the design of quantum computers. However, describing the non-equilibrium decoherence and population relaxation of a many-qubit system is non-trivial. No general model exists for this purpose. Classical noise models and microscopic noise models have yielded some success, but these formulations do not provide a general solution framework for a many-qubit system.

Classical noise models that describe the decoherence and population relaxation as exponential decays of the off-diagonal and diagonal components of the density matrix are widely used for the estimate of the error rates during quantum computation [11, 12], but generally these models lack quantum features that are important for quantum computing, such as the quantum interference effect.

Microscopic noise models based on the spin-boson Hamiltonian that explicitly include the linear couplings between the system and the bath degrees of freedom have provided valuable insights about decoherence effects [10, 11, 13]. Recently, the decoherence and gate performance of a quantum controlled-NOT (CNOT) gate operation for several different physical realizations has been studied based on such spin-boson type Hamiltonians [14, 15, 16, 17]. A number of different techniques has been developed to solve dynamics of microscopic Hamiltonians [18]. However, these methods are often complicated, and difficult to generalize for systems with more than two qubits. In addition, in many cases the exact form of the system-bath interactions is unknown, or the parameters are difficult to obtain experimentally, and the microscopic models are difficult to use in these cases.

The Bloch-Redfield formalism is generally used to study NMR spin-dynamics [19], and has been applied to study the dynamics of many-spin systems [20]. However, this formalism, while suitable

in NMR systems, is not always applicable in general qubit systems. Moreover, the Bloch-Redfield formalism is also known to violate the complete positivity of the reduced density operator at short times. To apply the Bloch-Redfield formalism to quantum computing, non-physical additional time intervals have to be inserted between the switching events [14, 15]. These extra time periods will result in the over-estimation of the degradation of the qubit systems.

Thus, generally speaking, a method that can be used to analyze the quality of a functional quantum circuit and capable of providing a quantitative result is still not available. In this work, we propose a stochastic Liouville equation approach to describe errors in quantum computations. This approach originates from the Haken-Strobl-Reineker (HSR) model first proposed by Haken and Strobl and later extended by Reineker in the 1970s to describe charge and energy transfer in organic crystals[21, 22, 23]. The HSR model is known to be able to capture the coherent and incoherent dynamics of quantum two-level systems. In this model, the system-bath interactions are taken into account by allowing the site energies and the off-diagonal matrix elements of the system to fluctuate over time. We generalize the idea of Haken and Strobl to describe a system of n qubits. The resulting stochastic Liouville equation is then solved to obtain a set of equations describing the dynamics of a general n qubit system. To demonstrate the applicability of our method, we study the effect of noise on quantum teleportation and a generic CNOT gate operation, and then compare our results with previous work. We show that our model can reproduce the main results obtained previously by using microscopic model Hamiltonians. The limitations and possible extensions of our semiclassical model are also discussed.

II. THE STOCHASTIC LIOUVILLE EQUATION APPROACH

Previous work on the study of the population relaxation and decoherence of qubit systems is usually based on the spin-boson Hamiltonian, in which the qubits are coupled linearly to the bath degrees of freedom (the environment), and the bath is treated explicitly as a system of harmonic oscillators [10, 11, 18]. Due to the difficulty of applying the spin-boson model to multiple qubit systems, we take another approach. Instead of treating the bath explicitly, we follow the stochastic Liouville approach of the HSR model, and consider an effective Hamiltonian that treats the effect of the bath as a set of classical fluctuating fields acting on the system [21, 22, 23]. To describe the dynamics of an array of qubits under the influence of an external control field and environmental noise, we consider a system of n qubits, and start from a Hamiltonian with time independent and time dependent parts. The general Hamiltonian of the qubit system can be written as

$$\begin{aligned}
\mathbf{H}(t) &= \mathbf{H}_0 + \mathbf{h}(t) \\
&= \sum_{i,j=0}^{2^n-1} [H_{ij} + h_{ij}(t)] c_i^\dagger c_j,
\end{aligned} \tag{1}$$

where c_i^\dagger and c_i are the creation and annihilation operators for the i -th state of the 2^n basis set. The time independent part \mathbf{H}_0 describes the interactions between qubits, while the time dependent part $\mathbf{h}(t)$ describes the fluctuations of the interactions due to the coupling to the environment. For simplicity, we assume throughout this work that the external control fields are switched on and off instantaneously, and the interactions introduced by the external control fields are constant in time; this corresponds to a rectangular pulse. More realistic pulse shapes can be incorporated into our treatment without too much additional work. In addition, a sequence of different rectangular pulses can be divided into time periods with a constant external field in each of them, and then treated separately using a different time independent \mathbf{H}_0 for each time period. Considering only constant external control fields does not affect the generality of this model.

The time dependent part of the Hamiltonian describes the influences of the environment via fluctuations of the system energy. This term may include fluctuations from many different origins, such as the fluctuations of imperfect control fields, the fluctuations induced by the bath on the qubit excitation energy, the off-diagonal matrix element, and the inter-qubit interactions. Following Haken and Strobl [21], we consider the fluctuations as random Gaussian Markov processes with zero mean and δ -function correlation times:

$$\begin{aligned}
\langle h_{ij}(t) \rangle &= 0 \\
\langle h_{ij}(t) h_{kl}(t') \rangle &= R_{ij;kl} \cdot \delta(t - t')
\end{aligned} \tag{2}$$

Here the brackets $\langle \rangle$ represents the thermal average over all bath degrees of freedom, and the time independent correlation matrix element $R_{ij;kl}$ is a real number describing the correlations between $h_{ij}(t)$ and $h_{kl}(t')$. All $R_{ij;kl}$ elements form a 2^{2n} -dimensional correlation matrix \mathbf{R} . In addition, we have the following symmetry property of \mathbf{R} :

$$R_{ij;kl} = R_{ji;kl} = R_{ij;lk} = R_{ji;lk} = R_{kl;ij} \tag{3}$$

The value of $R_{ij;kl}$ depends on the strength of the coupling to the environment; therefore, it is a measure of the noisiness of the environment. The δ -function correlation in time corresponds to

the limit of fast bath modulations, which assumes that the relaxation time of the bath is much larger than the characteristic time of the system. Therefore, this model should be valid at high temperature limit. Also note that although the effect of the temperature can be included by considering temperature dependent correlation matrix elements, there is no explicit temperature dependence in this model. We will discuss the consequences of this assumption and the applicability of this model in more detail in Section V.

The time independent part of the Hamiltonian \mathbf{H}_0 and the correlation matrix \mathbf{R} determine the dynamics of the system. The values of \mathbf{H}_0 and \mathbf{R} depend on the setup of the physical system, the various types of noise considered, and the nature of the bath. Note that in the HSR model, the system is limited to the one exciton subspace, and the matrix \mathbf{H}_0 and \mathbf{R} can be obtained directly. However, in our n -qubit system, all 2^n states must be considered, and how to determine \mathbf{H}_0 and \mathbf{R} is less obvious. In the following sections, we provide explicit examples of \mathbf{H}_0 and \mathbf{R} for systems describing quantum teleportation and generic quantum gates. Generalization of the procedure to determine \mathbf{H}_0 and \mathbf{R} for a general n -qubit system should be straightforward. Throughout this section we will only use the generic forms of \mathbf{H}_0 and \mathbf{R} to derive the equation of motion that describes the time evolution of the n -qubit system under the influence of noise.

The dynamics of the system is described by the stochastic Liouville equation ($\hbar = 1$)

$$\dot{\rho}(t) = -i[\mathbf{H}(t), \rho(t)],$$

where $\rho(t)$ is the density matrix of the system at time t . Using the statistical properties of $\mathbf{h}(t)$ [Eq. (2)] and the symmetry property of the correlation functions [Eq. (3)], we can compute the exact equation of motion for the averaged density matrix elements of the system by applying the second order generalized cumulant expansion method to average over all fluctuations. The result we obtain is in a simple form:

$$\begin{aligned} \frac{d}{dt} \tilde{\rho}_{\alpha\beta} = & -i \sum_j H_{\alpha j} \tilde{\rho}_{j\beta} + i \sum_j \tilde{\rho}_{\alpha j} H_{j\beta} \\ & - \frac{1}{2} \sum_{k,l} R_{lk;k\beta} \tilde{\rho}_{\alpha l} - \frac{1}{2} \sum_{k,l} R_{lk;k\alpha} \tilde{\rho}_{l\beta} + \sum_{k,l} R_{\beta l;k\alpha} \tilde{\rho}_{kl}, \end{aligned} \quad (4)$$

where all the summations are over all 2^n state indices. In addition, we have defined the averaged density matrix of the system, $\tilde{\rho}(t) = \langle \rho(t) \rangle$. In Eq. (4), the dynamics of the averaged density matrix can be separated into a coherent part, due to \mathbf{H}_0 , and an incoherent part, due to \mathbf{R} . The dissipation of the system is governed by incoherent dynamics, and is related to the elements of the fluctuation correlation matrix \mathbf{R} . Notice that the form of Eq. (4) is similar to the form of

the widely used Redfield equation, with the relaxation matrix elements given by the corresponding $R_{ij;kl}$ terms in the equation [24].

Eq. (4) forms a system of 2^{2n} linear ordinary differential equations (ODE). Given the values of H_{ij} and $R_{ij;kl}$, the ODE system can be solved efficiently to yield the time dependent averaged density matrix $\tilde{\rho}(t)$. In fact, in most one qubit and two qubit systems, the equations can be solved analytically, and the analytical formula for $\tilde{\rho}(t)$ can be obtained. In general, we can calculate \mathbf{H}_0 and \mathbf{R} from the Hamiltonian of the system and the correlations between fluctuations introduced by the environment. Once we have \mathbf{H}_0 and \mathbf{R} , it is then trivial to solve Eq. (4) to yield a $\tilde{\rho}(t)$ that fully describes the dynamics of the n-qubit system. This procedure is straightforward, and can be used to study the effect of noise in complex quantum computations. We demonstrate the applications of this model on the study of the effect of noise on quantum teleportation and general quantum two qubit gates in the next two sections.

III. DISSIPATION IN QUANTUM TELEPORTATION

Since first proposed by Bennett *et al.* in 1993 [25], the concept of "quantum teleportation" has received much attention. By exploiting the entangled nature of an Einstein-Podolsky-Rosen (EPR) pair, a sender can transmit the quantum state of a qubit to a receiver, without physically transferring the qubit through space. In this section, we will apply our stochastic Liouville approach to study the effect of noise on quantum teleportation.

A. Quantum teleportation

We first consider the ideal scenario of teleporting one qubit from Alice to Bob. Suppose Alice and Bob share a EPR pair, labeled as qubit a and b , emitted from an EPR pair source, and Alice wants to teleport qubit c in state $|\psi\rangle = c_0|0\rangle + c_1|1\rangle$ to Bob. The EPR pair source emits two entangled qubits in one of the four Bell states at time $t = 0$, and then the two qubits are sent through separate channels C_a and C_b to Alice and Bob, respectively. After receiving qubit a , Alice performs a Bell-state measurement on her qubits (a and c), and sends the outcome of her measurement to Bob through a classical channel. Alice's measurement projects qubit b onto one of the four corresponding states, i.e. $\mathbf{I} \cdot (c_0|0\rangle_b + c_1|1\rangle_b)$, $\sigma_z \cdot (c_0|0\rangle_b + c_1|1\rangle_b)$, $\sigma_x \cdot (c_0|0\rangle_b + c_1|1\rangle_b)$, and $i\sigma_y \cdot (c_0|0\rangle_b + c_1|1\rangle_b)$. Bob then applies the corresponding inverse transformation (\mathbf{I} , σ_z , σ_x , and $-i\sigma_y$, respectively) to recover his qubit in the state $|\psi\rangle$.

In practice, errors can happen during the quantum teleportation from several origins: (1) the noise in the quantum channels C_a and C_b , (2) the degradation of qubit c after the preparation, (3) the imperfect Bell-state measurement performed by Alice, (4) the further degradation of qubit b when transmitting the result of Bell-state measurement through the classical channel, (5) the imperfect unitary transformations performed by Bob. Here, we only consider the first situation where channel C_a and C_b are noisy, and focus on the errors due to the degradation of entanglement. We assume all other operations are done perfectly. This means that result obtained in the following represents a lower bound on the errors in the quantum teleportation.

B. Effect of noise on a pair of entangled qubits

To study the degradation of a pair of entangled qubits, we consider the effective Hamiltonian describing two uncorrelated qubits a and b :

$$\begin{aligned}
\mathbf{H} &= \mathbf{H}_a + \mathbf{H}_b \\
&= \sum_{n=a,b} \varepsilon_n(t) \cdot \sigma_z^{(n)} + \sum_{n=a,b} J_n(t) \cdot \sigma_x^{(n)} \\
&= \sum_{n=a,b} [\varepsilon_n + \delta\varepsilon_n(t)] \cdot \sigma_z^{(n)} + \sum_{n=a,b} [J_n + \delta J_n(t)] \cdot \sigma_x^{(n)},
\end{aligned} \tag{5}$$

where $\sigma_z^{(n)}$ and $\sigma_x^{(n)}$, $n = a, b$ are Pauli spin operators on qubit a and b ; $2\varepsilon_a$ ($2\varepsilon_b$) is the averaged energy splitting between the $|0\rangle$ and $|1\rangle$ states of qubit a (b); J_a (J_b) is the averaged off-diagonal matrix element for qubit a (b); $\delta\varepsilon_a(t)$ ($\delta\varepsilon_b(t)$) is the time-dependent fluctuating part of the diagonal energy for qubit a (b); $\delta J_a(t)$ ($\delta J_b(t)$) is the time-dependent fluctuating part of the off-diagonal matrix element for qubit a (b). Following the assumption made in Section II, we regard $\delta\varepsilon_n(t)$ and $\delta J_n(t)$, $n = a, b$ as Gaussian Markov processes fully described by their first two moments:

$$\begin{aligned}
\langle \delta\varepsilon_n(t) \rangle &= \langle \delta J_n(t) \rangle = 0, \\
\langle \delta\varepsilon_n(t) \delta\varepsilon_m(t') \rangle &= \gamma_0^n \cdot \delta_{nm} \delta(t - t'), \\
\langle \delta J_n(t) \delta J_m(t') \rangle &= \gamma_1^n \cdot \delta_{nm} \delta(t - t'), \\
\langle \delta\varepsilon_n(t) \delta J_m(t') \rangle &= 0,
\end{aligned} \tag{6}$$

where γ_0^a (γ_0^b) describes the strength of the diagonal energy fluctuations of qubit a (b); γ_1^a (γ_1^b) describes the strength of the off-diagonal matrix element fluctuations of qubit a (b). Clearly, γ_0^a and γ_0^b are related to the system-bath interactions involving σ_z system operators, and γ_1^a and γ_1^b

are related to the interactions involving σ_x system operators. These phenomenological parameters can be estimated experimentally [23, 26]. Notice that we treat the correlation between qubit a and b independently, because in quantum teleportation, the two EPR qubits are sent through different channels to two distantly separated places, thus the two qubits are coupled to distinct baths. In addition, we assume the diagonal and off-diagonal fluctuations are not correlated.

To simplify our computations, we choose to study the dynamics of the system in the Bell-state basis. The four Bell states are defined as

$$\begin{aligned} |B_1\rangle &= \frac{1}{\sqrt{2}}(|0\rangle_a|0\rangle_b + |1\rangle_a|1\rangle_b), \\ |B_2\rangle &= \frac{1}{\sqrt{2}}(|0\rangle_a|0\rangle_b - |1\rangle_a|1\rangle_b), \\ |B_3\rangle &= \frac{1}{\sqrt{2}}(|0\rangle_a|1\rangle_b + |1\rangle_a|0\rangle_b), \\ |B_4\rangle &= \frac{1}{\sqrt{2}}(|0\rangle_a|1\rangle_b - |1\rangle_a|0\rangle_b), \end{aligned}$$

where subscript a, b labels the state of different qubits. For convenience, hereafter we will use the notation that use the first digit to denote the state of qubit a , and the second digit to denote the state of qubit b , i.e. $|1\rangle_a|1\rangle_b \equiv |11\rangle$. The Hamiltonian for the two qubit system [Eq. (5)] in the Bell-state basis is

$$\mathbf{H} = \begin{bmatrix} 0 & \varepsilon_a + \varepsilon_b + h_{12}(t) & J_a + J_b + h_{13}(t) & 0 \\ \varepsilon_a + \varepsilon_b + h_{21}(t) & 0 & 0 & J_b - J_a + h_{24}(t) \\ J_a + J_b + h_{31}(t) & 0 & 0 & \varepsilon_a - \varepsilon_b + h_{34}(t) \\ 0 & J_b - J_a + h_{42}(t) & \varepsilon_a - \varepsilon_b + h_{43}(t) & 0 \end{bmatrix}, \quad (7)$$

where the nonzero transformed time-dependent matrix elements are:

$$\begin{aligned} h_{12}(t) &= h_{21}(t) = \delta\varepsilon_a(t) + \delta\varepsilon_b(t), \\ h_{13}(t) &= h_{31}(t) = \delta J_a(t) + \delta J_b(t), \\ h_{24}(t) &= h_{42}(t) = \delta J_b(t) - \delta J_a(t), \\ h_{34}(t) &= h_{43}(t) = \delta\varepsilon_a(t) - \delta\varepsilon_b(t). \end{aligned} \quad (8)$$

From Eq. (6) and Eq. (8), we can easily compute the correlation matrix \mathbf{R} of the system. In this case, \mathbf{R} has only 32 nonzero elements that can be represented by the following 6 irreducible elements:

$$\begin{aligned}
R_{12;12} &= \gamma_0^a + \gamma_0^b, \\
R_{12;34} &= \gamma_0^a - \gamma_0^b, \\
R_{13;13} &= \gamma_1^a + \gamma_1^b, \\
R_{13;23} &= \gamma_1^b - \gamma_1^a, \\
R_{24;24} &= \gamma_1^a + \gamma_1^b, \\
R_{34;34} &= \gamma_0^a + \gamma_0^b.
\end{aligned} \tag{9}$$

Other nonzero elements of \mathbf{R} can be obtained using the symmetry property of \mathbf{R} (Eq. (3)). Plugging the correlation matrix elements Eq. (7)] and the time-independent Hamiltonian matrix elements [Eq. (9)] into Eq. (4), we obtain the equation of motion for the averaged density matrix of the system, $\tilde{\rho}(t)$.

In the limit of zero averaged Hamiltonian matrix elements, $\varepsilon_n = J_n = 0$, the equation of motion for the diagonal density matrix elements are decoupled from those for the off-diagonal density matrix elements. Therefore, the dynamics of a system initially in one of the four Bell states (i.e. the initial density matrix has only non-zero diagonal elements) can be fully described by the equations for the diagonal density matrix elements:

$$\begin{aligned}
\frac{d}{dt}\tilde{\rho}_{11}(t) &= \Gamma_0 \cdot [\tilde{\rho}_{22}(t) - \tilde{\rho}_{11}(t)] + \Gamma_1 \cdot [\tilde{\rho}_{33}(t) - \tilde{\rho}_{11}(t)], \\
\frac{d}{dt}\tilde{\rho}_{22}(t) &= \Gamma_0 \cdot [\tilde{\rho}_{11}(t) - \tilde{\rho}_{22}(t)] + \Gamma_1 \cdot [\tilde{\rho}_{44}(t) - \tilde{\rho}_{22}(t)], \\
\frac{d}{dt}\tilde{\rho}_{33}(t) &= \Gamma_0 \cdot [\tilde{\rho}_{44}(t) - \tilde{\rho}_{33}(t)] + \Gamma_1 \cdot [\tilde{\rho}_{11}(t) - \tilde{\rho}_{33}(t)], \\
\frac{d}{dt}\tilde{\rho}_{44}(t) &= \Gamma_0 \cdot [\tilde{\rho}_{33}(t) - \tilde{\rho}_{44}(t)] + \Gamma_1 \cdot [\tilde{\rho}_{22}(t) - \tilde{\rho}_{44}(t)],
\end{aligned} \tag{10}$$

where we have defined $\Gamma_0 = (\gamma_0^a + \gamma_0^b)$, and $\Gamma_1 = (\gamma_1^a + \gamma_1^b)$. These equations have the form of a system of kinetic equations involving four states, and, clearly, Γ_0 and Γ_1 have the meaning of the degradation rate constants. The symmetric form of Eq. (10) suggests that all four states are equivalent dynamically, hence we expect the degradation rates of the systems initially in any of the four Bell states are equal. In this limit, the results of the teleportation based on different Bell-state channels are the same. Later we will show that this is only true when $\varepsilon_n = J_n = 0$ and the two qubits are coupled to distinct baths.

Eq. (10) also shows that a system of two qubits initially in one of the maximumly entangled states degrades into a statistical mixture of the four Bell states. Assuming that the system is initially in the state $|B_1\rangle$ and stays in the noisy quantum channels for a time period t , the density

matrix for the entangled qubits Alice and Bob obtained can be represented as the statistical mixture

$$\tilde{\rho}(t) = \tilde{\rho}_{11}(t) \cdot |B_1\rangle\langle B_1| + \tilde{\rho}_{22}(t) \cdot |B_2\rangle\langle B_2| + \tilde{\rho}_{33}(t) \cdot |B_3\rangle\langle B_3| + \tilde{\rho}_{44}(t) \cdot |B_4\rangle\langle B_4|. \quad (11)$$

The populations can be obtained by solving Eq. (10) with the initial condition $\rho_0 = |B_1\rangle\langle B_1|$:

$$\begin{aligned} \tilde{\rho}_{11}(t) &= \frac{1}{4} + \frac{1}{4}e^{-2\Gamma_0 t} + \frac{1}{4}e^{-2\Gamma_1 t} + \frac{1}{4}e^{-2(\Gamma_0+\Gamma_1)t}, \\ \tilde{\rho}_{22}(t) &= \frac{1}{4} - \frac{1}{4}e^{-2\Gamma_0 t} + \frac{1}{4}e^{-2\Gamma_1 t} - \frac{1}{4}e^{-2(\Gamma_0+\Gamma_1)t}, \\ \tilde{\rho}_{33}(t) &= \frac{1}{4} + \frac{1}{4}e^{-2\Gamma_0 t} - \frac{1}{4}e^{-2\Gamma_1 t} - \frac{1}{4}e^{-2(\Gamma_0+\Gamma_1)t}, \\ \tilde{\rho}_{44}(t) &= \frac{1}{4} - \frac{1}{4}e^{-2\Gamma_0 t} - \frac{1}{4}e^{-2\Gamma_1 t} + \frac{1}{4}e^{-2(\Gamma_0+\Gamma_1)t}. \end{aligned} \quad (12)$$

From Eq. (12), the fidelity of the entangled pair, defined as the overlap between the initial density matrix ρ_0 and the density matrix at time t , can be calculated:

$$F_e(t) = \mathbf{Tr} \rho_0 \tilde{\rho}(t) = \frac{1}{4} + \frac{1}{4}e^{-2\Gamma_0 t} + \frac{1}{4}e^{-2\Gamma_1 t} + \frac{1}{4}e^{-2(\Gamma_0+\Gamma_1)t}. \quad (13)$$

Eq. (13) shows that when Γ_0 and Γ_1 are both non-zero, the fidelity $F_e(\infty) = \frac{1}{4}$ in the long time limit. When either Γ_0 or Γ_1 is zero, $F_e(\infty) = \frac{1}{2}$. This result indicates that if we can somehow transform the system and minimize either the diagonal energy fluctuations or the off-diagonal matrix element fluctuations, the original quantum state can be better preserved. In addition, Eq. (13) can be used to compute a critical time scale beyond which the degraded entanglement can not be purified by any entanglement purification method [27]. The fidelity required by a successful entanglement purification process, $F_e(t) > 0.5$, corresponds to a critical time t_c where $F_e(t_c) = \frac{1}{2}$. For any high-fidelity quantum teleportation to be possible, the EPR pair should not be allowed to stay in the noisy channels for a time period longer than t_c . t_c also defines the critical distance for possible high-fidelity quantum teleportation, given the noise of the channels described by the parameters Γ_0 and Γ_1 .

C. Outcome of teleportation

Now we can use the result in the previous section to study the outcome of teleporting a qubit c in state $|\psi\rangle = c_0|0\rangle + c_1|1\rangle$ from Alice to Bob. We assume the traveling time that the EPR pair spends in the noisy channels is t , and the averaged energy ε_n and off-diagonal matrix elements J_n for both qubits are very small so that the limit of $\varepsilon_n = J_n = 0$, $n = a, b$ can be applied. After receiving the degraded EPR pair described by Eq. (11), Alice and Bob then perform the Bell-state measurement and corresponding unitary transformation to complete the teleportation. Assuming

that all measurements and unitary transformations are carried out perfectly and do not introduce more error, the teleportation outcome that Bob obtains is

$$\rho'(t) = \begin{bmatrix} \frac{1}{2} + \frac{1}{2}(|c_0|^2 - |c_1|^2) \cdot e^{-2\Gamma_1 t} & \frac{c_0 c_1^* + c_0^* c_1}{2} \cdot e^{-2\Gamma_0 t} + \frac{c_0 c_1^* - c_0^* c_1}{2} \cdot e^{-2(\Gamma_0 + \Gamma_1)t} \\ \frac{c_0 c_1^* + c_0^* c_1}{2} \cdot e^{-2\Gamma_0 t} + \frac{c_0^* c_1 - c_0 c_1^*}{2} \cdot e^{-2(\Gamma_0 + \Gamma_1)t} & \frac{1}{2} + \frac{1}{2}(|c_1|^2 - |c_0|^2) \cdot e^{-2\Gamma_1 t} \end{bmatrix}. \quad (14)$$

This result is similar to the result for the dissipation of a two level system in the HSR model [23, 26]. Notice that the decoherence depends on the total diagonal fluctuations, $\Gamma_0 = \gamma_0^a + \gamma_0^b$, and the population relaxation depends on the total off-diagonal fluctuations, $\Gamma_1 = \gamma_1^a + \gamma_1^b$. Clearly, noise in both channels affect the teleportation outcome additively. In fact, the outcome is exactly the same as if the teleported qubit is transferred physically from Alice to Bob through the noisy channel C_a and C_b , although the qubit Bob receives has never traveled through channel C_a physically.

The fidelity of teleportation as a function of the traveling time t is

$$F_{tele}(t) = \frac{1}{2} + \frac{1}{2}(c_0^* c_1 + c_0 c_1^*)^2 e^{-2\Gamma_0 t} + \frac{1}{2}(|c_0|^2 - |c_1|^2)^2 e^{-2\Gamma_1 t} - \frac{1}{2}(c_0^* c_1 - c_0 c_1^*)^2 e^{-2(\Gamma_0 + \Gamma_1)t}. \quad (15)$$

The fidelity of teleportation decreases monotonically from 1 to $\frac{1}{2}$ as the traveling time t increases. At the long time limit, the fidelity approaches $\frac{1}{2}$, which means the result of the quantum teleportation is a half-half mixture of $|0\rangle$ and $|1\rangle$ states, i.e. information about $|\psi\rangle$ is totally lost. This result is in agreement with recent studies on the effect of noise on quantum teleportation [28].

Eq. (15) provides a simple interpretation for the phenomenological parameter Γ_0 and Γ_1 : Γ_0 is the total decay rate for the real part of the coherence, and Γ_1 is the total population relaxation rate. Recall that γ_0^n , $n = a, b$ is defined using the second moment of the diagonal energy fluctuation $\delta\varepsilon_n(t)$, $n = a, b$ (coupling involving σ_z) and γ_1^n , $n = a, b$ is defined using the second moment of the off-diagonal matrix element fluctuation $\delta J_n(t)$, $n = a, b$ (coupling involving σ_x). We see clearly the effects of different types of noise: the diagonal fluctuations introduce phase shifts that only affect the coherence of the qubit; the off-diagonal fluctuations introduce coupling between the two states and result in population transfer. Note that the decay of the imaginary part of the coherence depends on both diagonal and off-diagonal fluctuations. In the terminology of quantum computing, phase-shift errors are caused by the diagonal energy fluctuations, bit-flip errors are caused by the off-diagonal matrix element fluctuations, and the change in the σ_y component are due to both types of fluctuations. Previous studies on the dissipation of qubits using spin-boson types of Hamiltonian give similar results for the effects of different types of system-bath interactions [10, 11, 13]. Our

model gives direct relationships between the phenomenological parameters describing the strength of the fluctuations and the dissipation rates. In addition, our model can take into account the effects of both types of fluctuations *simultaneously*, which is different from most error models used previously.

D. Nonzero averaged matrix elements

When the time-independent part of the Hamiltonian contains nonzero matrix elements, i.e. $\varepsilon_n \neq 0$ or $J_n \neq 0$, $n = a, b$, the exact analytical expression for $\tilde{\rho}(t)$ is not generally available. In addition, the effect of diagonal energy fluctuations no longer can be clearly distinguished from the effect of off-diagonal matrix element fluctuations, both population relaxation and decoherence depend on γ_0^n and γ_1^n , $n = a, b$. More importantly, the four Bell states no longer decay at the same rate, and we can see the effect of the coherent dynamics depending on the value of the averaged energy and off-diagonal matrix elements. In the weakly-damped regime where the averaged Hamiltonian matrix elements are larger than the strength of the noise, the dynamics of a pair of entangled qubits exhibits coherent oscillating behavior. These oscillations can lead to errors of the quantum teleportation. Figure 1 shows the fidelity of the four Bell states as a function of traveling time at $\varepsilon_a = \varepsilon_b = 1$, $J_a = J_b = 0.5$, $\gamma_0^a = \gamma_0^b = 0.1$, and $\gamma_1^a = \gamma_1^b = 0.1$. The different oscillating behavior of the Bell states can be understood by considering the time-independent part of the Hamiltonian. From Eq. (5), all the nonzero time-independent matrix elements are

$$\begin{aligned} \langle B_1 | \mathbf{H}_0 | B_2 \rangle &= \langle B_2 | \mathbf{H}_0 | B_1 \rangle = \varepsilon_a + \varepsilon_b, \\ \langle B_1 | \mathbf{H}_0 | B_3 \rangle &= \langle B_3 | \mathbf{H}_0 | B_1 \rangle = J_a + J_b, \\ \langle B_2 | \mathbf{H}_0 | B_4 \rangle &= \langle B_4 | \mathbf{H}_0 | B_2 \rangle = J_b - J_a, \\ \langle B_3 | \mathbf{H}_0 | B_4 \rangle &= \langle B_4 | \mathbf{H}_0 | B_3 \rangle = \varepsilon_a - \varepsilon_b. \end{aligned}$$

These matrix elements govern the coherent transition between the Bell states, and result in the oscillating behavior of the dynamics. In Fig. 1, the fidelity of the $|B_4\rangle$ state decays monotonically as t increases, because both matrix elements couple this state to the other states, $J_b - J_a$ and $\varepsilon_a - \varepsilon_b$, are zero for the parameters used. This also explains why the fidelity of the $|B_4\rangle$ state provides an upper bound on the fidelity of other Bell states in Fig. 1. The state that is coupled most weakly to other states decay most slowly.

In the regime where the averaged Hamiltonian matrix elements are smaller than the strength of the noise, the system is overdamped and no oscillating behavior can be observed. Figure 2

shows the fidelity of the four Bell states at $\varepsilon_a = \varepsilon_b = 0.1$, $J_a = J_b = 0.05$, $\gamma_0^a = \gamma_0^b = 0.1$, and $\gamma_1^a = \gamma_1^b = 0.1$. In this regime, all Bell states degrade monotonically as the traveling time increases.

The fidelity of the EPR pair used in the quantum teleportation is directly related to the fidelity of teleportation. Therefore, the above discussion can be directly applied to the fidelity of teleportation performed using different Bell states. When $\varepsilon_n \neq 0$ or $J_n \neq 0$, $n = a, b$, the fidelity of the teleportation behaves differently when different Bell states are used. To achieve the best result for the teleportation, we have to choose the Bell state that is coupled most weakly to other states. In general, $\varepsilon_n > 0$, $n = a, b$ and J_a and J_b have the same sign, thus $|B_4\rangle$ state will have the weakest coupling. The singlet $|B_4\rangle$ state is the preferred EPR state for the quantum teleportation.

[Fig. 1]

[Fig. 2]

E. Effect of collective bath

We have studied the dissipation of two entangled qubits each coupled to a distinct bath, which is the typical situation relevant for the quantum teleportation. Another interesting case is when the two qubits are coupled to a common bath. In this case, we use the Hamiltonian of Eq. (5); the difference in the state of the bath is reflected by different correlation functions for the stochastic processes. When the two qubits are coupled to a common bath, the first two moments can be represented as

$$\begin{aligned}
 \langle \delta\varepsilon_n(t) \rangle &= \langle \delta J_n(t) \rangle = 0, \\
 \langle \delta\varepsilon_n(t) \delta\varepsilon_m(t') \rangle &= \gamma_0 \cdot \delta(t - t'), \\
 \langle \delta J_n(t) \delta J_m(t') \rangle &= \gamma_1 \cdot \delta(t - t'), \\
 \langle \delta\varepsilon_n(t) \delta J_m(t') \rangle &= 0,
 \end{aligned} \tag{16}$$

where γ_0 describes the strength of the diagonal fluctuations; γ_1 describes the strength of the off-diagonal fluctuations. Note that because the qubits are coupled to a common bath, the fluctuations on different qubits are correlated. From Eq. (8) and Eq. (16), we can derive the correlation matrix \mathbf{R} for the system in the Bell-state basis. In this collective bath limit, \mathbf{R} has only 8 nonzero elements that can be represented by the following 2 irreducible elements:

$$\begin{aligned}
 R_{12;12} &= 4\gamma_0, \\
 R_{13;13} &= 4\gamma_1.
 \end{aligned} \tag{17}$$

Using Eq. (17), we can derive the equation of motion for the dynamics of two qubits coupled to a common bath. In the limit of zero averaged Hamiltonian matrix elements ($\varepsilon_n = J_n = 0$, $n = a, b$), we obtain a simple result for the populations in the four Bell states:

$$\begin{aligned}\frac{d}{dt}\tilde{\rho}_{11}(t) &= 4\gamma_0 \cdot [\tilde{\rho}_{22}(t) - \tilde{\rho}_{11}(t)] + 4\gamma_1 \cdot [\tilde{\rho}_{33}(t) - \tilde{\rho}_{11}(t)], \\ \frac{d}{dt}\tilde{\rho}_{22}(t) &= 4\gamma_0 \cdot [\tilde{\rho}_{11}(t) - \tilde{\rho}_{22}(t)], \\ \frac{d}{dt}\tilde{\rho}_{33}(t) &= 4\gamma_1 \cdot [\tilde{\rho}_{11}(t) - \tilde{\rho}_{33}(t)], \\ \frac{d}{dt}\tilde{\rho}_{44}(t) &= 0.\end{aligned}\tag{18}$$

Eq. (18) describes the dynamics for a system of two qubits coupled to a common bath in the Bell-state basis. Interestingly, the population in the $|B_4\rangle$ state, $\tilde{\rho}_{44}(t)$, is invariant in time. In addition, when only diagonal energy fluctuations exist ($\gamma_1 = 0$), the population in the $|B_3\rangle$ state is also invariant; when only off-diagonal matrix element fluctuations exist ($\gamma_0 = 0$), the population in the $|B_2\rangle$ state is invariant. Compared to the result of two qubits coupled to distinct baths [see Eq.(10)], Eq. (18) shows that the fluctuations interfere constructively for the $|B_1\rangle$ state leading to a faster decay rate, but destructively for the $|B_4\rangle$ state. This result can be understood easily in our stochastic model. In our model, the effect of environment on the system is represented by a fluctuating field, and the interaction Hamiltonian for the two qubits is $\mathbf{H}_{int} = \sigma_i^{(a)} \cdot V_a(t) + \sigma_i^{(b)} \cdot V_b(t)$ ($i = x, z$; a and b are labels for different qubits). When the two qubits are coupled to a common bath, $V_a(t) = V_b(t)$, we can factorize the interaction into the form $\mathbf{H}_{int} = (\sigma_i^{(a)} + \sigma_i^{(b)}) \cdot V_a(t)$. Therefore, any state $|\phi\rangle$ that satisfies $\langle\phi|\sigma_i^{(a)} + \sigma_i^{(b)}|\phi\rangle = 0$ does not interact with the fluctuating field, and is invariant to the noise. We can see that $\langle B_3|\sigma_z^{(a)} + \sigma_z^{(b)}|B_3\rangle = 0$ and $\langle B_4|\sigma_z^{(a)} + \sigma_z^{(b)}|B_4\rangle = 0$, thus both the $|B_3\rangle$ and $|B_4\rangle$ states are not affected by phase-shifting noise; $\langle B_2|\sigma_x^{(a)} + \sigma_x^{(b)}|B_2\rangle = 0$ and $\langle B_4|\sigma_x^{(a)} + \sigma_x^{(b)}|B_4\rangle = 0$, thus both the $|B_2\rangle$ and $|B_4\rangle$ states are not affected by bit-flipping noise. This effect of the collective bath has been verified experimentally [29], and studied in theoretical works related to the ideas of “quantum error-avoiding codes” [30, 31] and “decoherence-free subspaces” [32, 33]. Duan *et al.* have shown similar result using a Hamiltonian that explicitly includes the linear coupling terms between the system and the boson bath [31, 34]. The agreement indicates that our simple stochastic model can handle both the independent and the collective bath properly.

Recently, Kumar and Pandey have studied the effect of noise on quantum teleportation [28]. They applied two different models, a stochastic model and a spin-boson type model, to this problem, and studied the relative teleportation efficiencies of the Bell states. Their main result is that for the simple stochastic model, the four Bell states are equivalent, but for the second model in which

the effect of environment is considered explicitly, the $|B_4\rangle$ state is least affected by the noise. We obtain a similar conclusion using the stochastic Liouville equation approach. Based on our result, we understand that the $|B_4\rangle$ state is the least affected state because of the assumption of a collective bath, not because the effect of bath is considered microscopically. Like spin-boson type models, a simple stochastic model when treated correctly can provide the same result, and gives a simple picture for the effect of a collective bath versus a localized bath.

IV. ERRORS IN QUANTUM CNOT GATE

Qubits and quantum gates are the basic elements of quantum computing. A quantum circuit that performs a particular quantum operation can be expressed as a composition of elementary quantum gates [35]. In fact, quantum circuits can be constructed using one- and two-qubit gates as basic building blocks. For example, the quantum CNOT gate together with all one-qubit quantum gates form such a set of universal quantum gates [36]. In reality, quantum computations are performed by subjecting an array of qubits under a sequence of control fields that control the Hamiltonian of the qubit system and result in specific quantum gate operations. Therefore, we consider the process of quantum computation as preparing the qubit system in the initial state, then performing programmed control fields on the qubits in a sequence of time steps, and finally measuring the output in the working basis.

To understand the effect of noise on general quantum computations and help the implementation of quantum computers, we need a model that can be used to describe the decoherence and population relaxation for a system of qubits subjected to external control fields. The decoherence and gate performance of a CNOT gate on various types of physical realizations have been studied in Refs. [14, 15, 16, 17, 37]. In particular, Thorwart and Hnggi investigated the decoherence and dissipation for a generic CNOT gate operation using the numerical *ab initio* technique of the quasiadiabatic-propagator path integral (QUAPI). They demonstrated that this numerical method is capable of describing the full time-resolved dynamics of the two-qubit system in the presence of noise. To our knowledge, so far, the QUAPI method is the most sophisticated method that has been applied to study the decoherence during a CNOT gate operation. In this section, we apply the stochastic Liouville equation approach to study the same generic CNOT operation investigated by Thorwart and Hnggi, and show that our model yields similar results. In general, our model is easier to extend to many qubit systems than the QUAPI method, and can incorporate the effects of noise from different sources at the same time.

A. A generic model for 2-qubit quantum gates

In a physical system, a quantum gate can be expressed by a Hamiltonian with terms representing the control fields that result in the gate operation. Consider a elementary step in a quantum gate operation where the control Hamiltonian is switched on, a generic Hamiltonian describing the constant external fields and the time-dependent fluctuations (noise) for a two-qubit system can be written as

$$\begin{aligned}
 \mathbf{H}(t) &= \sum_{n=a,b} [\varepsilon_n + \delta\varepsilon_n(t)] \cdot \sigma_z^{(n)} + \sum_{n=a,b} [J_n + \delta J_n(t)] \cdot \sigma_x^{(n)} \\
 &\quad + [g + \delta g(t)] \cdot (\sigma_+^{(a)} \sigma_-^{(b)} + \sigma_-^{(a)} \sigma_+^{(b)}), \\
 &\equiv \mathbf{H}_0 + \mathbf{h}(t)
 \end{aligned} \tag{19}$$

where the two qubits are labeled as qubit a and qubit b ; the first two terms comprise the Hamiltonian for two non-interacting qubits considered in Eq. (5); the last term represents the inter-qubit interaction with $\sigma_{\pm}^{(n)} = (\sigma_x^{(n)} \mp i\sigma_y^{(n)})$, $n = a, b$; g and $\delta g(t)$ are the time-independent and time-dependent fluctuating part of the inter-qubit coupling. The controllable fields are represented by the values of ε_n , J_n , $n = a, b$, and g . Quantum gates can be implemented by switching these fields on and off in a controlled manner. Notice that the XY type of coupling is adopted in our model Hamiltonian. This interaction is just an illustrative example, and does not account for all the possible interactions in a specific realization of solid-state devices. The real form of the inter-qubit interaction term depends on the controllable interactions available for each individual physical implementation. Nevertheless, our model can handle the other types of interactions as well, and we expect that the model Hamiltonian we use here can reproduce the same general physical behavior as other two-qubit Hamiltonians.

From Eq. (19), we can write down the time-independent part of the Hamiltonian in the standard basis $\{|00\rangle, |01\rangle, |10\rangle, |11\rangle\}$:

$$\mathbf{H}_0 = \begin{bmatrix} \varepsilon_a + \varepsilon_b & J_b & J_a & 0 \\ J_b & \varepsilon_a - \varepsilon_b & g & J_a \\ J_a & g & \varepsilon_b - \varepsilon_a & J_b \\ 0 & J_a & J_b & -\varepsilon_a - \varepsilon_b \end{bmatrix}, \tag{20}$$

and the time-dependent part of the Hamiltonian is

$$\mathbf{h}(t) = \begin{bmatrix} \delta\varepsilon_a(t) + \delta\varepsilon_b(t) & \delta J_b(t) & \delta J_a(t) & 0 \\ \delta J_b(t) & \delta\varepsilon_a(t) - \delta\varepsilon_b(t) & \delta g(t) & \delta J_a(t) \\ \delta J_a(t) & \delta g(t) & \delta\varepsilon_b(t) - \delta\varepsilon_a(t) & \delta J_b(t) \\ 0 & \delta J_a(t) & \delta J_b(t) & -\delta\varepsilon_a(t) - \delta\varepsilon_b(t) \end{bmatrix}. \quad (21)$$

Furthermore, we assume the two qubits are close to each other in space, therefore, we consider the correlation functions suitable for two qubits coupled to a common bath. Again, we assume the fluctuations have zero mean and δ -function correlation times. The nonzero second moments are

$$\begin{aligned} \langle \delta\varepsilon_n(t) \delta\varepsilon_m(t') \rangle &= \gamma_0 \cdot \delta(t - t'), \\ \langle \delta J_n(t) \delta J_m(t') \rangle &= \gamma_1 \cdot \delta(t - t'), \\ \langle \delta g(t) \delta g(t') \rangle &= \gamma_2 \cdot \delta(t - t'), \end{aligned} \quad (22)$$

where γ_0 describes the strength of the diagonal energy fluctuations; γ_1 describes the strength of the off-diagonal matrix element fluctuations; γ_2 describes the strength of the fluctuations of the inter-qubit interactions. As we have shown in the previous section, these phenomenological parameters are related to the kinetic rate of each separate dissipative process, and can be easily measured experimentally. Also note that we directly include the inter-qubit coupling fluctuations, which corresponds to two-qubit flip-flop errors that are difficult to treat in the microscopic spin-boson type Hamiltonians.

Eq. (22) can be used to compute the elements of the correlation matrix \mathbf{R} . Using \mathbf{R} together with the averaged Hamiltonian matrix elements in Eq. (20), we can obtain the equation of motion describing the dynamics of the two-qubit system subjected to arbitrary one- and two-qubit control fields. As a result, we can study the dissipative dynamics of the qubit system during arbitrary gate operations. Although we only consider an operation done by a set of constant external fields, the behavior of more complicated gates that involve more than one step can be studied by combining the result for each elementary operations. In our model, the results for a set of universal quantum gates can be assembled to compute the results for a general quantum circuit.

B. The quantum CNOT gate

The quantum CNOT gate plays a central role in the quantum computation, because, as we noted above, the set of all one-qubit gates together with the CNOT gate is universal [36]. In the standard basis $\{|00\rangle, |01\rangle, |10\rangle, |11\rangle\}$, the ideal CNOT gate is represented as

$$U_{CNOT}^{ideal} = \begin{bmatrix} 1 & 0 & 0 & 0 \\ 0 & 1 & 0 & 0 \\ 0 & 0 & 0 & 1 \\ 0 & 0 & 1 & 0 \end{bmatrix}.$$

This gate operates on two qubits, and inverts the state of the second qubit if the first qubit is in the state $|1\rangle$. The CNOT gate cannot be constructed in one step using our model Hamiltonian. Instead, we must construct the CNOT gate using multiple elementary one- and two-qubit gates.

To begin with, we define the following one-qubit rotations on qubit a and b :

$$U_{nz}(\alpha) = e^{i\frac{\alpha}{2}\sigma_z^{(n)}}, \quad n = a, b,$$

$$U_{nx}(\alpha) = e^{i\frac{\alpha}{2}\sigma_x^{(n)}}, \quad n = a, b,$$

and the two-qubit operation:

$$U_j(\alpha) = e^{i\alpha(\sigma_+^{(a)}\sigma_-^{(b)} + \sigma_-^{(a)}\sigma_+^{(b)})}.$$

All these operations can be easily implemented using our model Hamiltonian [Eq. (19)] (with all control fields set to zero initially): $U_{nz}(\alpha)$, $n = a, b$, can be done by switching on $\varepsilon_n = -\varepsilon_0 \cdot \text{Sign}(\alpha)$ for a time period of $\tau = \frac{\alpha}{2\varepsilon_0}$; $U_{nx}(\alpha)$, $n = a, b$, can be done by switching on $J_n = -J_0 \cdot \text{Sign}(\alpha)$ for a time period of $\tau = \frac{\alpha}{2J_0}$; $U_j(\alpha)$ can be done by switching on $g = -g_0 \cdot \text{Sign}(\alpha)$ for a time period of $\tau = \frac{\alpha}{g_0}$; where the sign function $\text{Sign}(\alpha)$ returns -1 when $\alpha < 0$, and 1 when $\alpha > 0$. Using the corresponding averaged Hamiltonian \mathbf{H}_0 for each operations and the correlation matrix presented in the previous section, the equation of motion describing the dynamics of the two-qubit system subjected to any of these operations can be easily obtained. Actually, for arbitrary initial conditions, the analytical solution for the time-dependent two-qubit density matrix $\rho(t)$ during $U_{nx}(\alpha)$, $U_{nz}(\alpha)$, $n = a, b$, and $U_j(\alpha)$ operations are available in the Laplace domain, and can be used to study arbitrary quantum circuits composed by these three elementary operations.

The CNOT gate can be expressed by the following sequence of one- and two-qubit gate operations [9]:

$$U_{CNOT} = U_{bx}\left(\frac{\pi}{2}\right)U_{bz}\left(\frac{-\pi}{2}\right)U_{bx}(-\pi)U_j\left(\frac{-\pi}{2}\right)U_{ax}\left(\frac{-\pi}{2}\right)U_j\left(\frac{\pi}{2}\right)U_{bz}\left(\frac{-\pi}{2}\right)U_{az}\left(\frac{-\pi}{2}\right). \quad (23)$$

Table (I) lists the required control fields and time span to implement each step using our model Hamiltonian. In Table (I), we use ε_0 , J_0 , and g_0 to denote the strength of the controllable single-qubit bias, intra-qubit coupling, and inter-qubit XY interaction, respectively. In addition, we assume that the controllable field strengths and noise (defined by parameters γ_0 , γ_1 , and γ_2 as mentioned in the previous section) for the two qubits are identical. The value of these parameters should depend on the specific physical realization of the qubit systems. The total time required to perform the CNOT gate is $\tau_{cnot} = \pi/2\varepsilon_0 + \pi/J_0 + \pi/g_0$. For a typical energy scale of 1 meV (suitable for quantum dot qubits), the operation time is on the picosecond time scale.

[Table I]

Using the parameters listed in Table (I), we can calculate the time-dependent two-qubit density matrix $\rho(t)$ during CNOT operations under different noise conditions defined by γ_0 , γ_1 , and γ_2 . Figure 3 shows the time-resolved CNOT operation for two qubits initially in the $|11\rangle$ state. We set the strengths of the control fields equal to 1, i.e. $\varepsilon_0 = J_0 = g_0 = 1$. The ideal operation (solid line) starts at population 1 in the $|11\rangle$ state, and ends its total population in the $|10\rangle$ state, showing a successful CNOT operation. Three different noisy operations are shown in Fig. 3: (1) operation with the strength of the diagonal energy fluctuations $\gamma_0 = 0.05$ (dashed line), (2) operation with the strength of the off-diagonal matrix element fluctuations $\gamma_1 = 0.05$ (dash-dotted line), (3) operation with the strength of the inter-qubit coupling fluctuations $\gamma_2 = 0.05$ (dotted line). The effect of noise on the CNOT operation can be clearly seen. In previous work, Thorwart and Hnggi derived the same time-resolved CNOT operation result [15]. Our result is very close to their numerical *ab initio* QUAPI result. The agreement between our time-resolved result to the QUAPI result gives us confidence that our model captures the correct physics.

We use the gate fidelity and gate purity to characterize the performance of the CNOT gate. Other gate quantifiers including the quantum degree and entanglement capability are also calculated [38], but we do not show the results here because they follow the same trend as the gate fidelity and gate purity. In our formalism, the density matrix for the two qubits after the noisy CNOT operation, $\rho(\tau_{cnot})=U_{CNOT}\rho_0U_{CNOT}^\dagger$, can be calculated for any initial density matrix ρ_0 . Following Thorwart and Hnggi , we average the gate fidelity and gate purity over 16 initial states to account for the general performance of the CNOT gate. The 16 unentangled input states $|\psi_0^{ij}\rangle$, $i, j = 1, 2, 3, 4$ are defined as $|\psi_0^{ij}\rangle = |\phi_i\rangle_a \otimes |\phi_j\rangle_b$ with $|\phi_1\rangle = |0\rangle$, $|\phi_2\rangle = |1\rangle$, $|\phi_3\rangle = (|0\rangle + |1\rangle)/\sqrt{2}$, $|\phi_4\rangle = (|0\rangle + i|1\rangle)/\sqrt{2}$, and a, b denoting the state for different qubits. These

states span the Hilbert space for the two-qubit operations, and should give a reasonable result for the averaged effect [15, 38].

The gate fidelity is defined as the overlap between the ideal output and the output of the real gate operation. Using the 16 initial states, the averaged fidelity can be written as

$$F = \frac{1}{16} \sum_{i,j=1}^4 \langle \psi_{out}^{ij} | \rho_{CNOT}^{ij} | \psi_{out}^{ij} \rangle,$$

where we have defined the ideal CNOT output $|\psi_{out}^{ij}\rangle = U_{CNOT}^{ideal} |\psi_0^{ij}\rangle$, and the output of the real CNOT operation $\rho_{CNOT}^{ij} = U_{CNOT} |\psi_0^{ij}\rangle \langle \psi_0^{ij}| U_{CNOT}^\dagger$. The gate fidelity is a measure of how close the real operation is compared to the ideal operation. For a perfect gate operation, the gate fidelity should be 1.

Similarly, the averaged gate purity is defined as

$$P = \frac{1}{16} \sum_{i,j=1}^4 \text{Tr}((\rho_{CNOT}^{ij})^2).$$

The gate purity quantifies the effect of decoherence. For a perfect gate operation, the gate purity should be 1.

[Figure 3]

C. Dependence on the noise strength

The results of the averaged gate fidelity and gate purity as a function of the strength of each individual type of noise are shown in Fig. 4. For our generic study, we again set the strengths of all the control fields to 1, i.e. $\varepsilon_0 = J_0 = g_0 = 1$. Clearly, different types of noise cause different amount of errors. However, they all follow the same trend. The deviations of the gate fidelity and gate purity from the ideal values, i.e. $1 - F$ and $1 - P$, are sensitive to the strength of the noise, and saturate to 0.75 in the strong noise limit; the value 0.75 corresponds to a fully mixed state. In the weak noise regime, both $1 - F$ and $1 - P$ depend linearly on the noise strength, as expected [15, 16]. The proportionality constant in this case is ~ 10 . In fact, the proportionality constant depends on the strengths of the control fields, and reflects the total operation time required to complete the CNOT gate operation. As the strength of the control field increases, the total operation time decreases, and the qubits have less time to undergo the dissipative processes, resulting in less degradation. To minimize the effect of noise, we need to reduce the proportionality constant,

therefore, we will want to operate the device at the highest control fields possible. However, the situation will be different if increasing the strengths of the control fields will also introduce more noise. We will explicitly discuss the effect of the control-field strength in the next subsection.

From our results for $\varepsilon_0 = J_0 = g_0 = 1$, to achieve the threshold accuracy of the 0.999 99 level needed for arbitrary long quantum computations [39, 40, 41], one needs to keep the noise strength below the 10^{-6} level. Assuming a characteristic energy scale of 1 meV, this value corresponds to a decoherence time γ^{-1} in the μs scale, which provides a serious challenge for experimentalists working on the realization of solid-state quantum computers.

[Fig. 4]

The linear dependence of $1 - F$ and $1 - P$ on the noise strengths also indicates that the effect of *the same* type of noise is additive in the weak noise regime. To study the additivity of *different* types of noise, we calculate the averaged CNOT gate fidelity when different types of noise coexist at the same time. We define the total error of the CNOT gate operation E as the deviation of the gate fidelity from the ideal value:

$$E(\gamma_0, \gamma_1, \gamma_2) = 1 - F(\gamma_0, \gamma_1, \gamma_2), \quad (24)$$

where we have explicitly expressed the total error E as a function of the three different types of noise strengths: γ_0 , γ_1 , and γ_2 . In Fig. 5, we show the errors of the CNOT gate operation where the different types of noise coexist, and compare them to the total errors obtained by adding up the errors caused by the individual type of noise. Clearly, for all four situations considered, these two lines collapse in the weak noise regime. The results indicate that errors caused by different types of noise are additive in the small noise regime. In other words, the following identity holds in the small noise regime:

$$E(\gamma_0, \gamma_1, \gamma_2) = E(\gamma_0, 0, 0) + E(0, \gamma_1, 0) + E(0, 0, \gamma_2). \quad (25)$$

Eq. (25) justifies previous studies where different types of system-bath interactions are treated independently [15, 16].

[Fig. 5]

D. Dependence on the strength of the inter-qubit coupling

In the solid-state implementations of qubit devices, the achievable inter-qubit coupling (g_0 in our model) is usually weaker than other single-qubit interactions. Since the time required to finish a quantum gate operation is inverse proportional to the strength of the control field used, the weak interaction means long operation time, hence more errors. The two-qubit gate operations ($U_j(\alpha)$ in our model) is usually the bottleneck of quantum computation. In this section, we analyze the dependence of the quality of the quantum CNOT gate operation on the strength of the inter-qubit coupling g_0 .

If the strength of the inter-qubit coupling g_0 can be increased without introducing any extra disturbance on the system, then we expect operating the device in the strongest g_0 achievable will give the best result. However, physically, applying a stronger field also means introducing stronger noise due to the imperfectness of the field. In our model, this means stronger fluctuations on the inter-qubit XY interaction. The extra noise can be expressed in the value of the γ_2 term. To incorporate this effect, we allow γ_2 to depend on the strength of the inter-qubit coupling g_0 . Figure 6 shows the errors of the CNOT gate operation as a function of g_0 at $\gamma_0 = 0.001$, $\gamma_1 = 0.001$, $\varepsilon_0 = 1$, and $J_0 = 1$. Three different noise strength dependences are shown: (1) constant $\gamma_2 = 0.001$ (solid curve), (2) linear $\gamma_2 = 0.001 \cdot (1 + g_0)$ (dashed curve), and (3) quadratic $\gamma_2 = 0.001 \cdot (1 + g_0^2)$ (dash-dotted curve). The three curves show the same behavior in the small g_0 regime, in which the operation takes too much time and the system is fully degraded. As the strength of the coupling g_0 increases, the errors decrease due to the shorter operation time. When the strength of the coupling g_0 approaches the strengths of other control fields ($\varepsilon_0 = J_0 = 1$ in this case), the three curves start to show different behavior. For both constant and linear γ_2 , the errors generated by other operations ($U_{nz}(\alpha)$ and $U_{nx}(\alpha)$) dominate the errors of the CNOT gate operation, therefore, increasing g_0 gains nothing and the curve saturates. Our result for the constant γ_2 case is in agreement with the result obtained previously using the QUAPI method [15]. The situation is different when the strength of the noise depends on g_0 quadratically. For this case, the errors start to increase after $g_0 > 1$, because increasing the inter-qubit coupling g_0 introduces stronger noise that cannot be compensated by shorter operation times. Therefore, in the quadratic case, there exists an optimal g_0 for the gate operation.

[Fig. 6]

V. LIMITATIONS AND POSSIBLE EXTENSIONS

We have shown that the generalized HSR model is flexible for realistic physical devices. Applications of this model on the effect of noise on the quantum teleportation and CNOT gate operation give us similar results compared to previous studies based on microscopic models. In this section, we will briefly discuss the limitations and possible extensions of this stochastic Liouville equation approach.

A key step in the HSR model is to replace the microscopic system-bath interactions by stochastic processes. This procedure has permitted a full description of the dissipative dynamics of qubit systems and their response to the external fields. At the same time, we introduce phenomenological parameters to describe the strengths of fluctuations (γ_0 , γ_1 , and γ_2 in our model). These parameters have to be determined experimentally or computed using a separate microscopic model [22, 42, 43]. Generally, γ_0 , γ_1 , and γ_2 should depend on temperature and increase as temperature increases. However, our model lacks explicit temperature dependence for these parameters, thus cannot be used to study the temperature dependence of the qubit dynamics. Fortunately, these parameters are directly related to physically measurable quantities, and can be easily determined by experiments. In our model, γ_0 , γ_1 , and γ_2 correspond to the decoherence rate, population relaxation rate, and inter-qubit flip-flopping rate, respectively; all of them can be measured by one- and two-qubit experiments. In addition, recent theoretical studies on the temperature dependence of the quality of quantum CNOT gate operation suggest that the temperature dependence of the gate performance is weak [15, 16], which is reasonable in the weak coupling regime and the temperature range relevant to solid-state qubit systems.

The assumption of the fast modulation of the bath might be a more serious problem for the HSR model. The δ -function correlation time corresponds to an infinite fast decay of the bath correlations, which leads to incorrect short time dynamics and long time equilibrium populations. Palma *et al.* have studied the decoherence of a qubit and shown that the dynamics exhibits a “quiet” and a “quantum” regime at short times, and a “thermal” regime at long times [11]. The HSR model assumes that the bath relaxes infinitely fast, thus neglects the dynamics of the system before bath relaxation takes place. Although the HSR model cannot predict the short time dynamics correctly, we expect the physics for longer operations important for quantum computing are reasonably well captured. The delta function correlation can be replaced by an exponential function in time, and the extended model for a dichotomic process has been solved exactly without further assumptions [44, 45, 46, 47]. It will be interesting to apply these extended models to quantum computations

and compare the results with the δ correlation function results.

The white noise assumption in the HSR model also corresponds to a bath with infinite temperature, therefore, the resulting equation of motion does not satisfy detailed balance at finite temperatures. As a consequence, the system always relaxes to equal populations regardless of the energy differences between the states. Extensions of the HSR model to solve this problem has been proposed in Ref. [43]. In quantum computing, we are mainly concerned about the dynamics of an unbiased qubit system, and even when a bias field is applied to the system to perform gate operations, the time period has to be short to avoid any population relaxation. Since we will only operate the quantum computer in the time scale that the population relaxation is negligible, we expect the violation of the detailed balance condition will not cause serious problems for applications related to quantum computing.

The stochastic representation for the dynamics of a quantum two-level system has been investigated in Refs. [48] and [49]. The correspondence between the phenomenological parameters describing the stochastic field (γ_0 and γ_1 in this work) and the two-level system microscopic quantities are also studied. The stochastic approximation is found to be able to reproduce the results by Leggett *et al.* for the spin-boson model [18]. Our results presented confirm this observation. In general, the stochastic Liouville equation approach presented in this work is applicable in the weak system-bath interaction limit relevant to quantum computations.

VI. CONCLUSION

In this work, we present a stochastic Liouville equation approach that provides a simple way to evaluate the effect of noise in quantum computations. This approach is generalized from the HSR model. Using an effective system Hamiltonian that includes the system-bath interactions as stochastic fluctuating terms with zero mean and delta function correlation times, we derived the exact equation of motion describing the dissipative dynamics for a system of n qubits. This generalized equation of motion is similar to the form of the widely used Redfield equation, with the relaxation matrix elements given by the corresponding correlation matrix elements.

We then applied this model to study the dissipative dynamics of a system of two independent qubits that mimics the EPR pair used in the quantum teleportation. We showed that the phenomenological parameters used in our model, i.e. γ_0 and γ_1 , correspond to the decoherence and population relaxation rate, respectively. To study the effect of noise on quantum teleportation, we calculated the fidelity of quantum teleportation. We found the effect of noise in the quantum

channels are additive, and the teleportation fidelity depends on the state of the teleported qubit. When the two EPR qubits are degenerate and have no intra-qubit coupling, the relative efficiencies of teleportation for the four Bell states are the same; otherwise, the singlet state $|B_4\rangle$ is the most efficient one. When the two qubits are coupled to the same bath (collective decoherence case), the $|B_1\rangle$ state is superdecoherent, while the $|B_4\rangle$ state is decoherence-free.

Furthermore, we studied a generic two-qubit Hamiltonian containing XY type inter-qubit interaction. The dissipative dynamics of a set of one- and two-qubit quantum gates were studied, and the results were then combined to calculate the averaged gate fidelity and gate purity for the quantum CNOT gate operation. The dependence of the quality of the quantum CNOT gate operation on the noise strength and the strength of the inter-qubit coupling were investigated. We found that the quality of the CNOT gate operation is sensitive to the noise strength and the strengths of the control fields. In addition, the effect of noise is additive regardless of its origin. We compared our results to Thorwart and Hnggi's results obtained by the numerical *ab initio* QUAPI technique. In general, our results are in good agreement with those obtained by the numerical QUAPI method.

We also discussed the limitations of the HSR type approach. The consequences due to the procedure of replacing the system-bath interactions by classical fluctuating fields and the assumption of the white noise were considered, and the possible extensions were noted. Generally, the application of HSR type model in the weak coupling regime that is relevant to quantum computing is justified.

Finally, we emphasize that the model presented in this work can be used to study the dissipative dynamics of a many-qubit system with direct inter-qubit coupling, imperfectness of the control field, and other many-qubit effects. The power of this method is in its simple physical interpretation of the parameters and dissipative dynamics. In addition, because of the δ -function correlation time assumed in the model, there is no time-ordering problem for the propagator computed using Eq. (4). The resulting propagator satisfies complete positivity, therefore no additional time period has to be inserted between switching events, as will be necessary for methods based on the Bloch-Redfield formalism. As a result, propagators computed for simple one- and two-qubit gates can be directly assembled to study the dissipative dynamics of more complicated quantum circuits. Since this model can handle noise that affects multiple qubits at the same time, e.g. the fluctuations in the XY type inter-qubit interaction that results in flip-flop errors, it will be very interesting to apply this method to analyze the behavior of a quantum circuit implementing quantum error-correcting or fault-tolerant codes under the influence of various multiple-qubit noise. We also expect this method to be applied to evaluate the quality of quantum circuits under realistic device

conditions. Such theoretical studies will be useful for the design and implementation of quantum computers.

Acknowledgments

This work has been partly supported by the National Science Foundation.

-
- [1] M. Nielsen and I. Chuang, *Quantum Computation and Quantum Information* (Cambridge University Press, 2000).
 - [2] I. Chuang, L. Vandersypen, X. Zhou, D. Leung, and S. Lloyd, *Nature* **393**, 143 (1998).
 - [3] I. Chuang, N. Gershenfeld, and M. Kubinec, *Phys. Rev. Lett.* **80**, 3408 (1998).
 - [4] L. Vandersypen, M. Steffen, G. Breyta, C. Yannoni, R. Cleve, and I. Chuang, *Phys. Rev. Lett.* **85**, 5452 (2000).
 - [5] L. Vandersypen, M. Steffen, G. Breyta, C. Yannoni, M. Sherwood, and I. Chuang, *Nature* **414**, 883 (2001).
 - [6] S. Gulde, M. Riebe, G. Lancaster, C. Becher, J. Eschner, H. Haffner, F. Schmidt-Kaler, I. Chuang, and R. Blatt, *Nature* **421**, 48 (2003).
 - [7] B. Kane, *Nature* **393**, 133 (1998).
 - [8] A. Imamoglu, D. Awschalom, G. Burkard, D. DiVincenzo, D. Loss, M. Sherwin, and A. Small, *Phys. Rev. Lett.* **83**, 4204 (1999).
 - [9] Y. Makhlin, G. Schon, and A. Shnirman, *Rev. Mod. Phys.* **73**, 357 (2001).
 - [10] W. Unruh, *Phys. Rev. A* **51**, 992 (1995).
 - [11] G. Palma, K.-A. Suominen, and A. Ekert, *Proc. R. Soc. Lond. A* **452**, 567 (1996).
 - [12] P. Knight, M. Plenio, and V. Vedral, *Philos. Trans. R. Soc. Lond. Ser. A-Math. Phys. Eng. Sci.* **355**, 2381 (1997).
 - [13] D. Walls and G. Milburn, *Phys. Rev. A* **31**, 2403 (1985).
 - [14] D. Loss and D. DiVincenzo, *Phys. Rev. A* **57**, 120 (1998).
 - [15] M. Thorwart and P. Hänggi, *Phys. Rev. A* **65**, 012309 (2002).
 - [16] M. Storz and F. Wilhelm, *Phys. Rev. A* **67**, 042319 (2003).
 - [17] M. Governale, M. Grifoni, and G. Schon, *Chem. Phys.* **268**, 273 (2001).
 - [18] A. Leggett, S. Chakravarty, A. Dorsey, M. Fisher, A. Garg, and W. Zwerger, *Rev. Mod. Phys.* **59**, 1 (1987).
 - [19] P. Argyres and P. Kelley, *Phys. Rev.* **134**, A98 (1964).
 - [20] C. P. Slichter, *Principles of Magnetic Resonance* (Springer Verlag, 1996).
 - [21] H. Haken and G. Strobl, *Z. Physik* **262**, 135 (1968).

- [22] H. Haken and P. Reineker, *Z. Physik* **249**, 253 (1972).
- [23] P. Reineker, *Exciton Dynamics in Molecular Crystals and Aggregates* (Springer-Verlag, Berlin, 1982).
- [24] A. Redfield, *Adv. Mag. Res.* **1**, 1 (1965).
- [25] C. Bennett, G. Brassard, C. Crepeau, R. Jozsa, A. Peres, and W. Wootters, *Phys. Rev. Lett.* **70**, 1895 (1993).
- [26] R. Silbey, *Ann. Rev. Phys. Chem.* **27**, 203 (1976).
- [27] C. Bennett, G. Brassard, S. Popescu, B. Schumacher, J. Smolin, and W. Wootters, *Phys. Rev. Lett.* **76**, 722 (1996).
- [28] D. Kumar and P. Pandey, *Phys. Rev. A* **68**, 012317 (2003).
- [29] P. Kwiat, A. Berglund, J. Altepeter, and A. White, *Science* **290**, 498 (2000).
- [30] P. Zanardi and M. Rasetti, *Phys. Rev. Lett.* **79**, 3306 (1997).
- [31] L. Duan and G. Guo, *Phys. Rev. Lett.* **79**, 1953 (1997).
- [32] D. Lidar, I. Chuang, and K. Whaley, *Phys. Rev. Lett.* **81**, 2594 (1998).
- [33] D. Bacon, D. Lidar, and K. Whaley, *Phys. Rev. A* **60**, 1944 (1999).
- [34] L. Duan and G. Guo, *Phys. Rev. A* **57**, 737 (1998).
- [35] D. DiVincenzo, *Phys. Rev. A* **51**, 1015 (1995).
- [36] A. Barenco, C. Bennett, R. Cleve, D. DiVincenzo, N. Margolus, P. Shor, T. Sleator, J. Smolin, and H. Weinfurter, *Phys. Rev. A* **52**, 3457 (1995).
- [37] A. Fowler, C. Wellard, and L. Hollenberg, *Phys. Rev. A* **67**, 012301 (2003).
- [38] J. Poyatos, J. Cirac, and P. Zoller, *Phys. Rev. Lett.* **78**, 390 (1997).
- [39] D. Aharonov and M. Ben-Or, in *Proceedings of the 29 Annual ACM Symposium on the Theory of Computing* (1997), pp. 176–188.
- [40] E. Knill, R. Laflamme, and W. Zurek, *Proc. R. Soc. London A* **454**, 365 (1998).
- [41] J. Preskill, *Proc. R. Soc. London A* **454**, 385 (1998).
- [42] S. Rackovsky and R. Silbey, *Mol. Phys.* **25**, 61 (1973).
- [43] V. Čápek, *Chem. Phys.* **171**, 79 (1993).
- [44] C. Warns, I. Barvik, and P. Reineker, *Phys. Rev. E* **57**, 3928 (1998).
- [45] V. Kraus and P. Reineker, *Phys. Rev. A* **43**, 4182 (1991).
- [46] M. Palenberg, R. Silbey, and W. Pfluegl, *Phys. Rev. B* **62**, 3744 (2000).
- [47] M. Palenberg, R. Silbey, C. Warns, and P. Reineker, *J. Chem. Phys.* **114**, 4386 (2001).
- [48] L. Accardi, S. Kozzyrev, and I. Volovich, *Phys. Rev. A* **56**, 2557 (1997).
- [49] Y. Kuzovlev, *JETP Lett.* **78**, 92 (2003).

TABLE I: Parameters of the model Hamiltonians used to perform the CNOT gate in 7 steps. The required control fields and time span for each step are listed. Note that we only list the nonzero field parameters.

No.	Operation	Control Fields	Time
1	$U_{bz}(\frac{-\pi}{2})U_{az}(\frac{-\pi}{2})$	$\varepsilon_a = \varepsilon_0, \varepsilon_b = \varepsilon_0$	$\tau_1 = \frac{\pi}{4\varepsilon_0}$
2	$U_j(\frac{\pi}{2})$	$g = -g_0$	$\tau_2 = \tau_1 + \frac{\pi}{2g_0}$
3	$U_{ax}(\frac{-\pi}{2})$	$J_a = J_0$	$\tau_3 = \tau_2 + \frac{\pi}{4J_0}$
4	$U_j(\frac{-\pi}{2})$	$g = g_0$	$\tau_4 = \tau_3 + \frac{\pi}{2g_0}$
5	$U_{bx}(-\pi)$	$J_b = J_0$	$\tau_5 = \tau_4 + \frac{\pi}{2J_0}$
6	$U_{bz}(\frac{-\pi}{2})$	$\varepsilon_b = \varepsilon_0$	$\tau_6 = \tau_5 + \frac{\pi}{4\varepsilon_0}$
7	$U_{bx}(\frac{\pi}{2})$	$J_b = -J_0$	$\tau_7 = \tau_6 + \frac{\pi}{4J_0}$

Figure Captions:

FIG. 1. Fidelity as a function of the traveling time for the Bell states in the coherent regime: $\varepsilon_a = \varepsilon_b = 1$, $J_a = J_b = 0.5$, $\gamma_0^a = \gamma_0^b = 0.1$, and $\gamma_1^a = \gamma_1^b = 0.1$.

FIG. 2. Fidelity as a function of the traveling time for the Bell states in the over-damped regime: $\varepsilon_a = \varepsilon_b = 0.1$, $J_a = J_b = 0.05$, $\gamma_0^a = \gamma_0^b = 0.1$, and $\gamma_1^a = \gamma_1^b = 0.1$.

FIG. 3. Tim-resolved CNOT gate operation on the $|11\rangle$ input state. Shown are the populations in the four basis states $\mathbf{P}_{ij}(t) = \langle ij|\rho(t)|ij\rangle$ as a function of time. The strengths of all the fields are set to 1 in the calculation, i.e. $\varepsilon_0 = J_0 = g_0 = 1$, and the corresponding time steps are defined in Table (I). We show the results for four different CNOT gate operations: (1) ideal operation without any noise (solid line), (2) operation with the strength of the diagonal fluctuations $\gamma_0 = 0.05$ (dashed line), (3) operation with the strength of the off-diagonal fluctuations $\gamma_1 = 0.05$ (dash-dotted line), (4) operation with the strength of the inter-qubit coupling fluctuations $\gamma_2 = 0.05$ (dotted line).

FIG. 4. Dependence of the errors in the CNOT gate operation on the noise strength. The deviations of the gate fidelity (upper panel) and gate purity (lower panel) from the ideal values are shown, i.e. $1 - F$ and $1 - P$. The effects of three types of noise are shown in both plots: (1) diagonal fluctuations represented by γ_0 (solid line), (2) off-diagonal fluctuations represented by γ_1 (dashed line), (3) inter-qubit fluctuations represented by γ_2 (dash-dotted line). The control-field strengths are set to $\varepsilon_0 = J_0 = g_0 = 1$.

FIG. 5. We show the error functions $E(\gamma_0, \gamma_1, \gamma_2)$ of the CNOT gate operation in situations where the different types of noise coexist (solid lines). For each case, the corresponding total errors obtained by adding up the errors caused by the individual types of noise is also shown (dotted lines). Four different combinations are compared: upper-left: $E(\Gamma, \Gamma, 0)$ vs. $E(\Gamma, 0, 0) + E(0, \Gamma, 0)$ (γ_0 and γ_1); upper-right: $E(0, \Gamma, \Gamma)$ vs. $E(0, \Gamma, 0) + E(0, 0, \Gamma)$ (γ_1 and γ_2); lower-left: $E(\Gamma, 0, \Gamma)$ vs. $E(\Gamma, 0, 0) + E(0, 0, \Gamma)$ (γ_0 and γ_2); lower-right: $E(\Gamma, \Gamma, \Gamma)$ vs. $E(\Gamma, 0, 0) + E(0, \Gamma, 0) + E(0, 0, \Gamma)$ (all types of noise). The strengths of all the control fields are set to 1, i.e. $\varepsilon_0 = J_0 = g_0 = 1$. We can clearly see that errors caused by different types of noise are additive in the small noise regime.

FIG. 6. Dependence of the errors in the CNOT gate operation on the strength of the inter-qubit coupling g_0 . Shown are the deviations of the gate fidelity from the ideal value for three types of γ_2 : (i) constant $\gamma_2 = 0.001$ (solid curve), (ii) linear $\gamma_2 = 0.001 \cdot (1 + g_0)$ (dashed curve), and (iii) quadratic $\gamma_2 = 0.001 \cdot (1 + g_0^2)$ (dash-dotted curve). Other parameters are set to $\gamma_0 = 0.001$, $\gamma_1 = 0.001$, $\varepsilon_0 = 1$, and $J_0 = 1$.

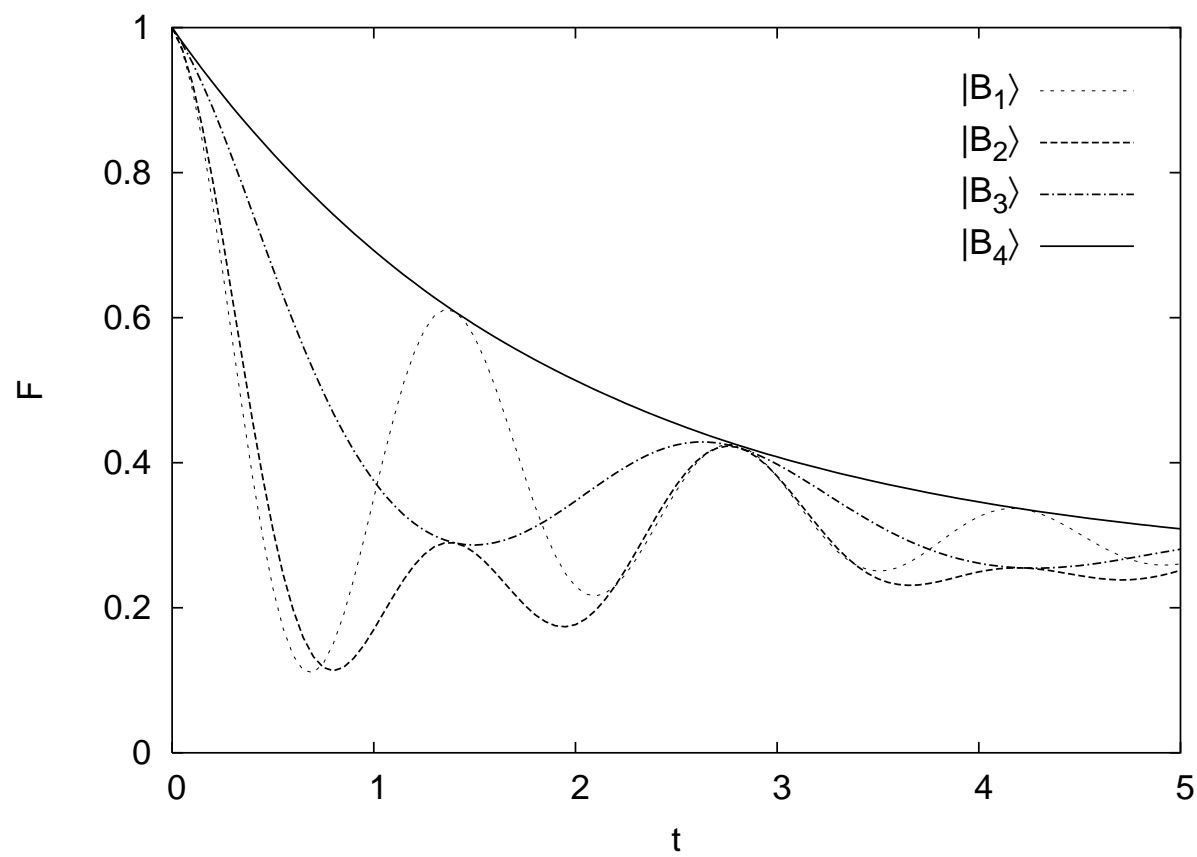


FIG. 1:

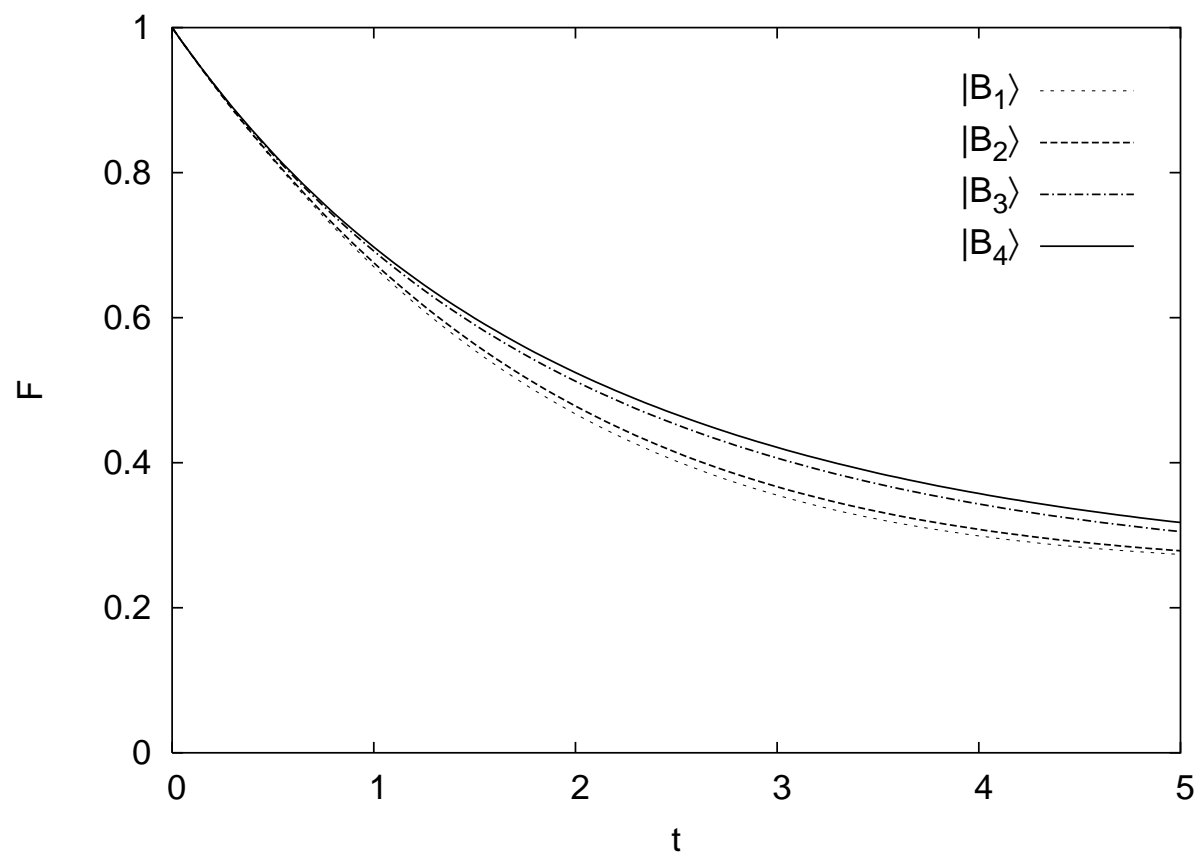


FIG. 2:

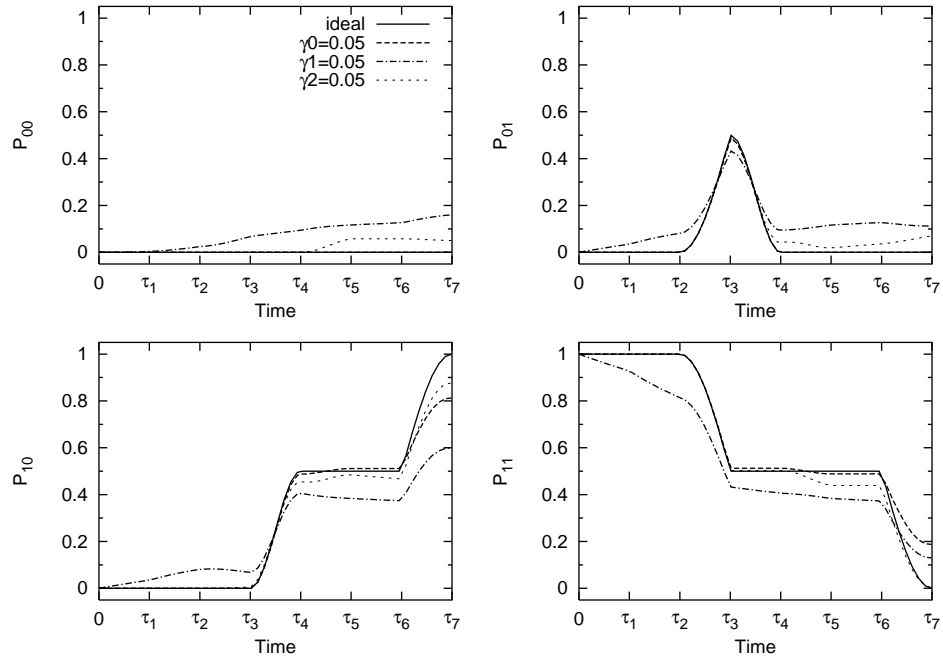


FIG. 3:

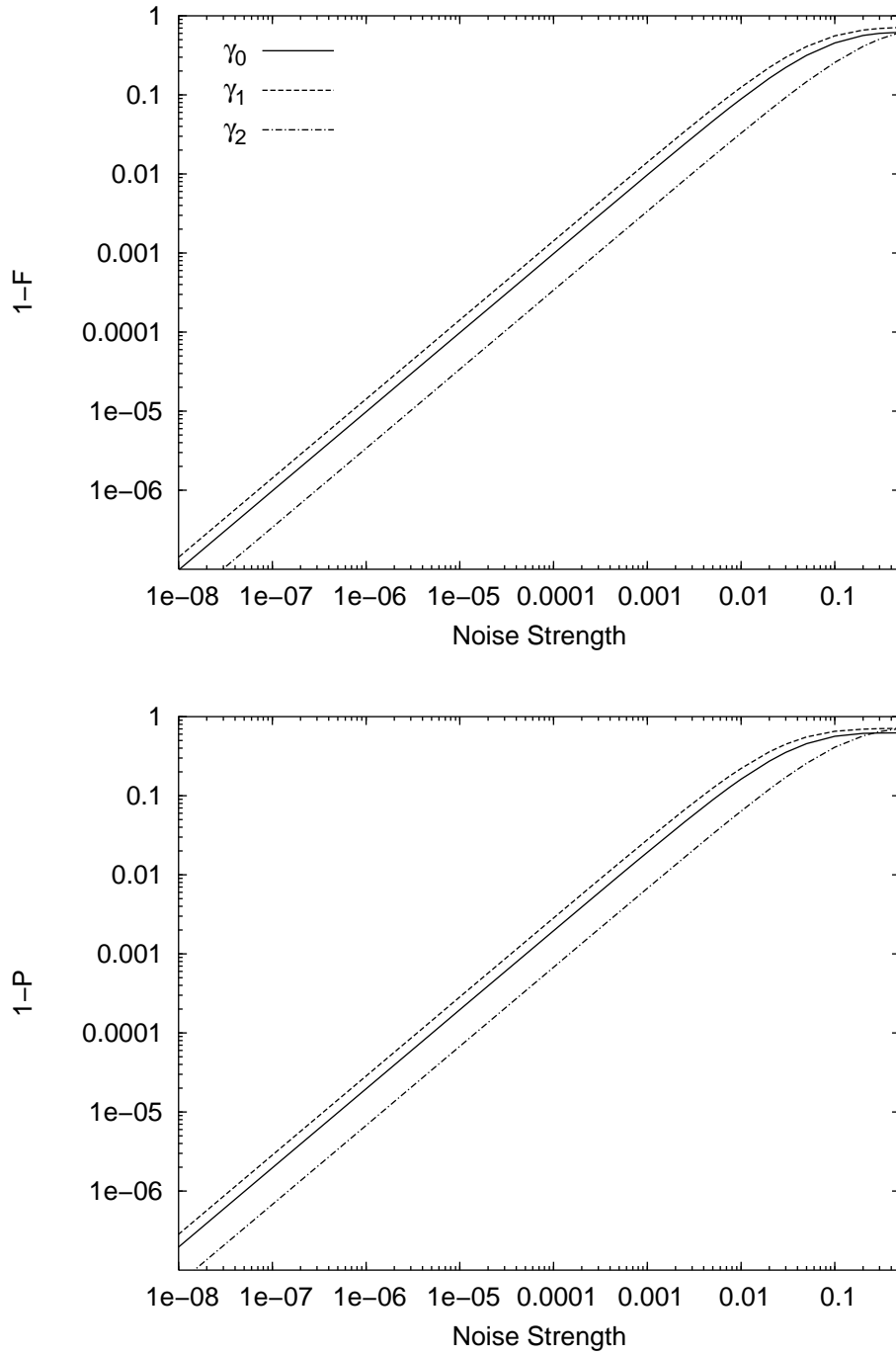


FIG. 4:

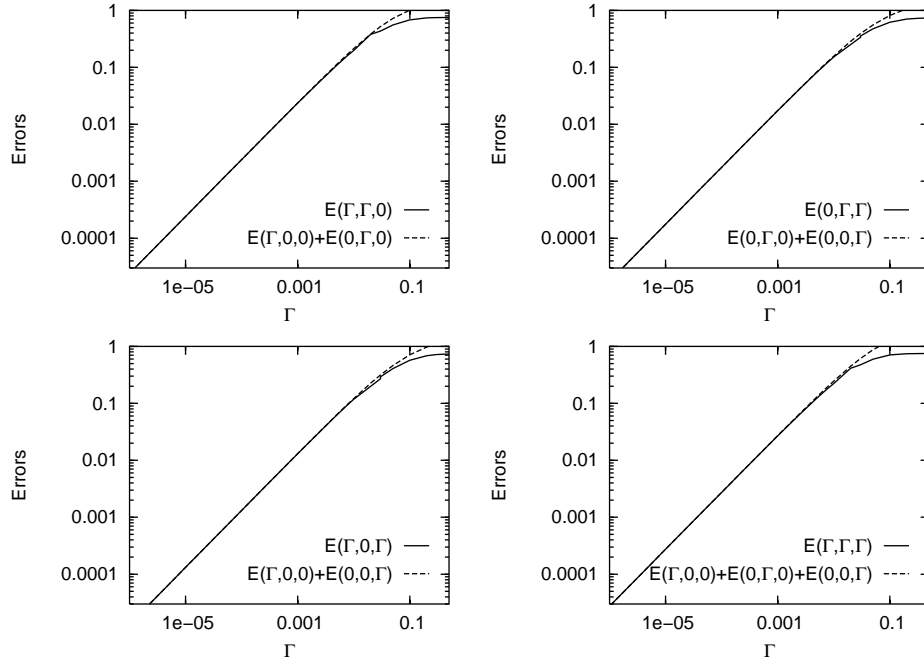


FIG. 5:

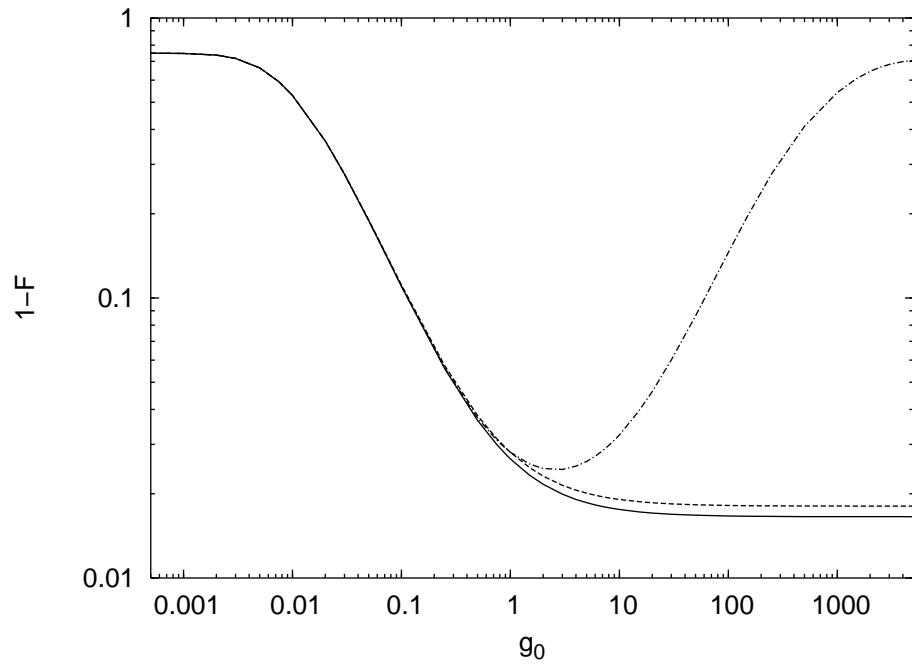


FIG. 6: